NUMERICAL SIMULATIONS OF COLLISIONS AND GRAVITATIONAL ENCOUNTERS IN SYSTEMS OF NON-IDENTICAL PARTICLES

H. SALO

Department of Astronomy, University of Oulu, Finland

(Received October 1, 1984)

Abstract. Numerical simulations of 200 mutually colliding non-identical particles indicate that the equipartition of random kinetic energy is possible only in systems having a narrow distribution of particle masses. Otherwise the random energy is concentrated on heavy particles. The form of the velocity distribution versus particle mass depends also on the elastic properties of the particles, and on the relative importance of the particle size. If the coefficient of restitution is a weakly decreasing function of impact velocity, a large difference in the equilibrium velocities of largest and smallest particles is possible. On the other hand, if the elasticity drops to a low level even in the small velocity regime, the dispersion of velocities is maintained by finite size and differential rotation, and the velocities of smallest particles are, at most, slightly larger than those of the largest ones. The results of simulations are consistent with the predictions of the collisional theory of non-identical particles (Hämeen-Anttila, 1984). The application to Saturn's rings indicates that the geometric thickness of cm-sized particles is of the order of 50 m in the rarefied regions of the rings. Without the gravitational encounters a thickness of about 30 m is derived. These estimations are made by using the latest measurements (Bridges *et al.*, 1984) for the restitution coefficient of icy particles.

1. Introduction

In the preliminary study of colliding non-identical particles (Salo and Lukkari, 1984; hereafter referred to as Paper I) the parameters determining the local equilibrium state of bimodal size-distributions were examined, whereas only a few simulations with a continuous distribution of sizes were performed. The present investigation concentrates on the latter type of systems, and in some simulations also gravitational encounters are taken into account. The results of the simulations are compared with recent analytical calculations (Hämeen-Anttila, 1984). In general, there is good agreement between the theoretical and numerical calculations. This justifies the extrapolation of results to a real system, such as the rarefied regions of Saturn's rings.

2. Method of Simulation

The simulation system is similar to that described in Paper I: it consists of 200 spherical, frictionless, mutually colliding particles, revolving in the gravitational field of a central body. The initial values of semi-major axes, a, are randomly chosen from the interval 0.8 to 1.2, while the eccentricities, ϵ, and inclinations, i, follow the Rayleigh-distribution. Other orbital elements are randomly distributed between 0 and 2π. The units of masses and radii are fixed by the above choice of semi-major axes, and by the condition $\gamma m = 1$,

Earth, Moon, and Planets **33** (1985) 189–200. 0167–9295/85.15.

where γ stands for the gravitational constant and m for the mass of the central body. With the adopted particle sizes, the mean optical thickness of the system is of the order of 0.01.

The method used in Paper I (see also Hämeen-Anttila and Lukkari, 1980) for the calculation of collisions is only applicable to Keplerian orbits. Therefore a different method, based on the Taylor expansions (Lukkari and Salo, 1984) was used in the simulations with self-gravitation. The computation of all mutual forces would be much too time consuming: instead of this the attraction between two particles was taken into account only if their distance was below a certain adjustable limit, typically about 0.1. This method eliminates the average self-gravitational field, but because of the low density this has no practical significance. A few separate calculations were made with an additional vertical force, simulating the conditions inside a dense homogenous self-gravitating disk.

For the the coefficient of restitution, α, the same model function was used as in Paper I, namely

$$\alpha = 1/(1 + |\mathbf{c}\cdot\mathbf{v}|/v_0), \quad \text{with} \quad v_0 = \text{const.}, \tag{1}$$

where $|\mathbf{c}\cdot\mathbf{v}|$ is the perpendicular component of the impact velocity. According to this relation $\alpha(\mathbf{v})$ is a decreasing function, as indicated by the recent laboratory measurements of impacts between icy particles at low temperatures (Bridges *et al.*, 1984).

3. Simulations with Two Particle Populations

Paper I describes two series of simulations in which the parameters affecting the local equilibrium values of eccentricities and inclinations were systematically studied. It was observed that both the ratio between particle masses, μ_1/μ_2, and the ratio between optical thicknesses, τ_1/τ_2, are important (subscript 1 refers to larger particles and 2 to smaller ones). A comparison with analytical results (Hämeen-Anttila, 1984) showed good agreement, unless μ_1/μ_2 was too large or τ_1/τ_2 too small. In simulations these limits correspond to a low total optical thickness, and later test runs revealed that the discrepancy was mostly due to the small number of simulation particles, leading to a non-random orientation of orbits. Because of finite computational accuracy this can lead to a formation of collisionless orbits, which are not taken into account in the statistical theory (Hämeen-Anttila and Lukkari, 1980). Due to this deficiency it was felt necessary to repeat some of the simulations of Paper I with more appropriate parameter values. In these new simulations (Figure 1) the discrepancy is avoided since the particles are larger.

Figure 1 depicts the results of simulations carried out with 40 large particles having the constant radius of 0.01, and with 160 small particles with $\sigma_2 = (\mu_2/\mu_1)^{1/3}\sigma_1$. The theoretical values of the steady-state eccentricities and inclinations are constructed by the same method as in Hämeen-Anttila (1984), except that the σ-terms of his equations are also included. Instead of plotting both $\sqrt{\overline{e^2}}$ and $\sqrt{\overline{i^2}}$ we only give their weighted mean

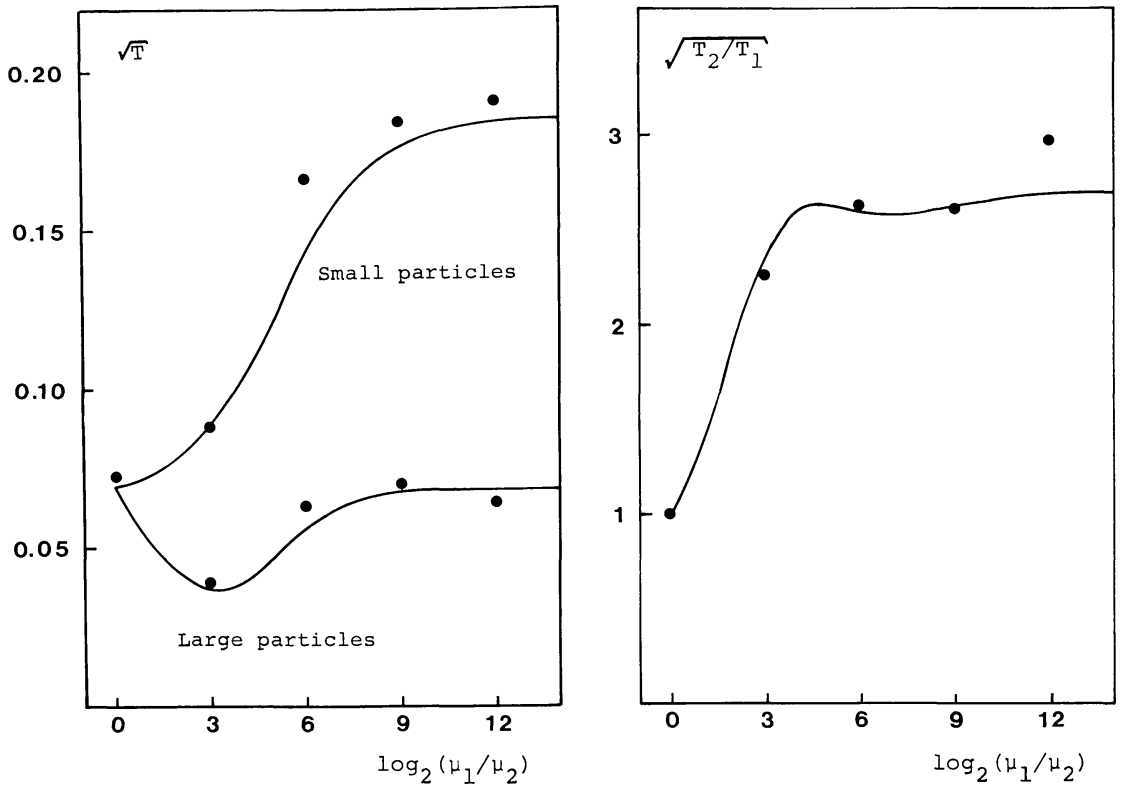

Fig. 1. The observed steady-state values of $\sqrt{T_1}$, $\sqrt{T_2}$, and $\sqrt{T_2/T_1}$, plotted as a function of μ_1/μ_2. The system consists of $N_1 = 40$ large and $N_2 = 160$ small particles, $\sigma_1 = 0.01$, and $v_0 = 0.15$. Theoretical curves are shown by solid lines.

$\sqrt{T}$, where $2T = (5/4)\overline{\epsilon^2} + \overline{i^2}$, represents the mean-square random velocity. The ratio $\sqrt{\overline{i^2}}/\sqrt{\overline{\epsilon^2}}$ is almost constant, being close to the theoretical value of 0.63. The simulation quantities are constructed as mean values for the whole system over the last 1000 impacts (of a total number of about 6000 impacts per simulation). The theoretical curves are calculated for the distance $r = 1$, and for the fixed initial values of the optical thickness. Thus the difference in the rate of radial spreading (Paper I) is ignored. In the simulations with large μ_1/μ_2 the final radial dispersion of smaller particles was sometimes nearly twice, compared to large ones. However, according to the theory this should lead only about a 10% difference in the $\sqrt{T_2/T_1}$ calculated for the initial and final relative densities.

The main difference between Figure 1 and the corresponding Figure 3 of Paper I is in the behaviour of large particles when $\mu_1/\mu_2 > 2^4$. According to the new simulations the influence of small particles on the equilibrium velocities of the large ones was negligible if $\mu_1/\mu_2 > 2^9$. This is seen from the close agreement of $\sqrt{T_1}$ with the equilibrium values of identical particles (corresponding to $\mu_1/\mu_2 = 1$). In the simulations of Paper I the velocity dispersion of large particles stayed at a much lower level, even when μ_1/μ_2 was as large as 2^{12}, but this was caused by the above-mentioned ordered orbits. The ratio between the velocity dispersions of both populations, measured in terms of $\sqrt{T_2/T_1}$, behaved in the same manner in both series of simulations. This is due to the fact that

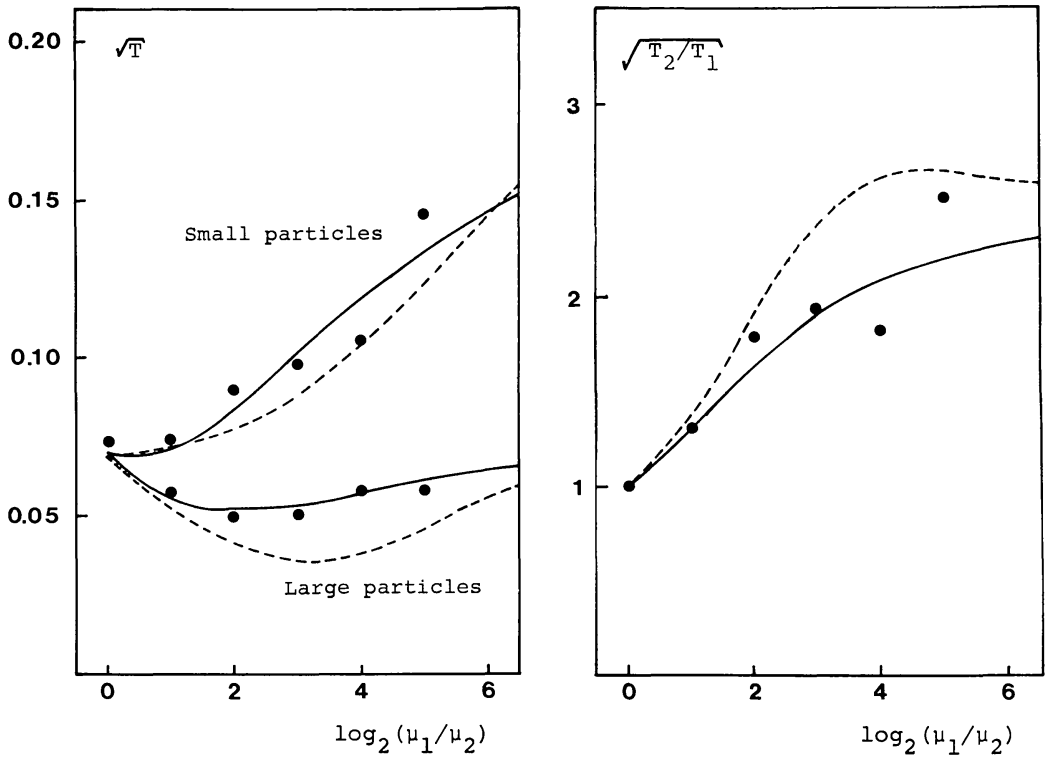

Fig. 2. Same as Figure 1 except that gravitational encounters are also taken into account, $\mu_1 = 2 \times 10^{-5}$. Theoretical curves are constructed both with (solid lines) and without (dashed lines) encounters.

the equilibrium velocities of smaller particles are determined by the impacts with large particles if μ_1/μ_2 is large, and thus in the previous simulations the ratio $\sqrt{T_2/T_1}$ was not affected by the reduced values of $\sqrt{T_2}$ and $\sqrt{T_1}$. Now the agreement between theory and simulations is good over the whole range of mass-ratios.

Figure 2 shows the behaviour of the simulation system if the gravitational encounters are also taken into account. The mass of the large particles was fixed to $\mu_1 = 2 \times 10^{-5}$, and thus the maximum mutual force between two large particles was 5% of the central force at unit distance. Due to the limited computational accuracy simulations were performed only with $\mu_1/\mu_2 < 2^6 (\sigma_1/\sigma_2 < 4)$. The program, based on Taylor expansions, accepts the impact if the distance of colliding bodies is within 5% of the sum of radii. For a small particle with $\sigma_2 = 0.25\,\sigma_1$ this would mean only about 20% accuracy, which is the maximum that was thought tolerable (in the program for Keplerian systems the accuracy is 1%, thus not leading to this problem until $\mu_1/\mu_2 > 10^3$). Typically, the inclusion of mutual gravitational interactions tends to decrease the difference of velocity dispersions.

Another series of encounter simulations was also made (Figure 3). In it the ratio μ_1/μ_2 was fixed to 8, while both μ_1 and μ_2 were varied. The theory follows the simulations until $\mu_1 \simeq 10^{-4}$. This upper limit is caused by an extensive formation of small local condensations, which are not included in the theoretical equations. The same

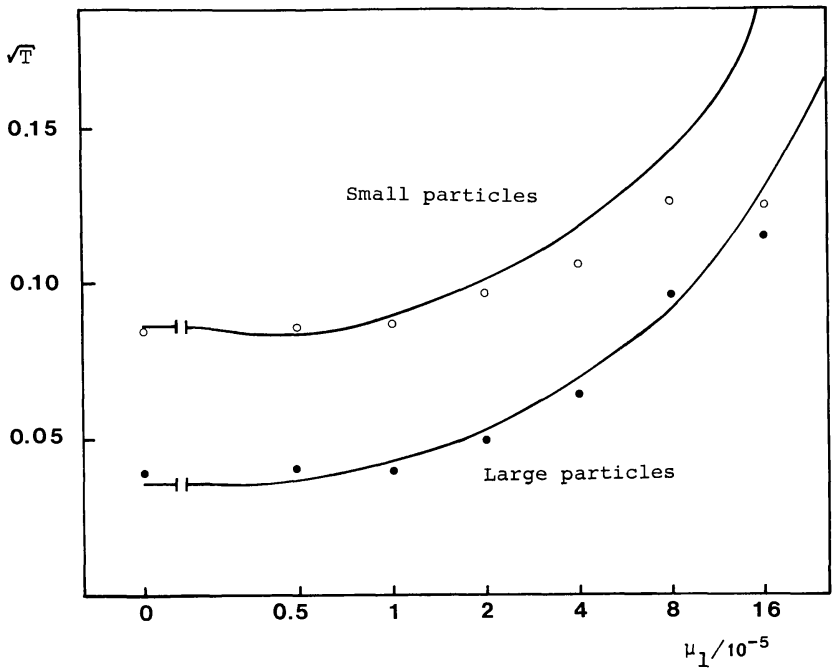

Fig. 3. Same as Figure 1, but μ_1 is used as a free variable while μ_1/μ_2 is fixed to 8.

phenomena was also seen in some previous simulations of identical particles (Lukkari and Salo, 1984) but it was now more pronounced.

The effects of the average self-gravitational field were studied in the same manner as in Lukkari and Salo's (1984) work on identical particles. An additional term, $kz^2/2$, $k = \text{const.}$, where z is the vertical distance from the mid-plane, was added to the central potential, corresponding to the mean field inside a uniform disk. This method, besides being much faster than the numerical evaluation of all the forces, also eliminates the excessive fluctuations in the actual field of relatively few simulation particles. According to the simulations, only inclinations are affected, as is also predicted by theoretical curves (Figure 4).

4. Simulations with a Continuous Distribution of Sizes

In Paper I some simulations were carried out with a power-law distribution of masses,

$$\mathrm{d}N/\mathrm{d}\mu \sim \begin{cases} \mu^{-(2+q)/3} & \text{if} \quad \mu_a \leqslant \mu \leqslant \mu_b \\ 0 \quad , \quad q = \text{const.}, & \text{if} \quad \mu < \mu_a \quad \text{or} \quad \mu > \mu_b. \end{cases} \tag{2}$$

With $q = 3$, an almost complete equipartition of random kinetic energy, measured by μT, was observed over the mass-range of $\mu_b/\mu_a = 32$ ($\sigma_b = 0.001$, and $v_0 = 0.05$). However, theoretical results (Hämeen-Anttila, 1984) indicate that the equipartition is not possible over a wide distribution of masses, but the random energy is strongly concentrated on the large particles. The distribution of μT is also likely to depend on the value of q,

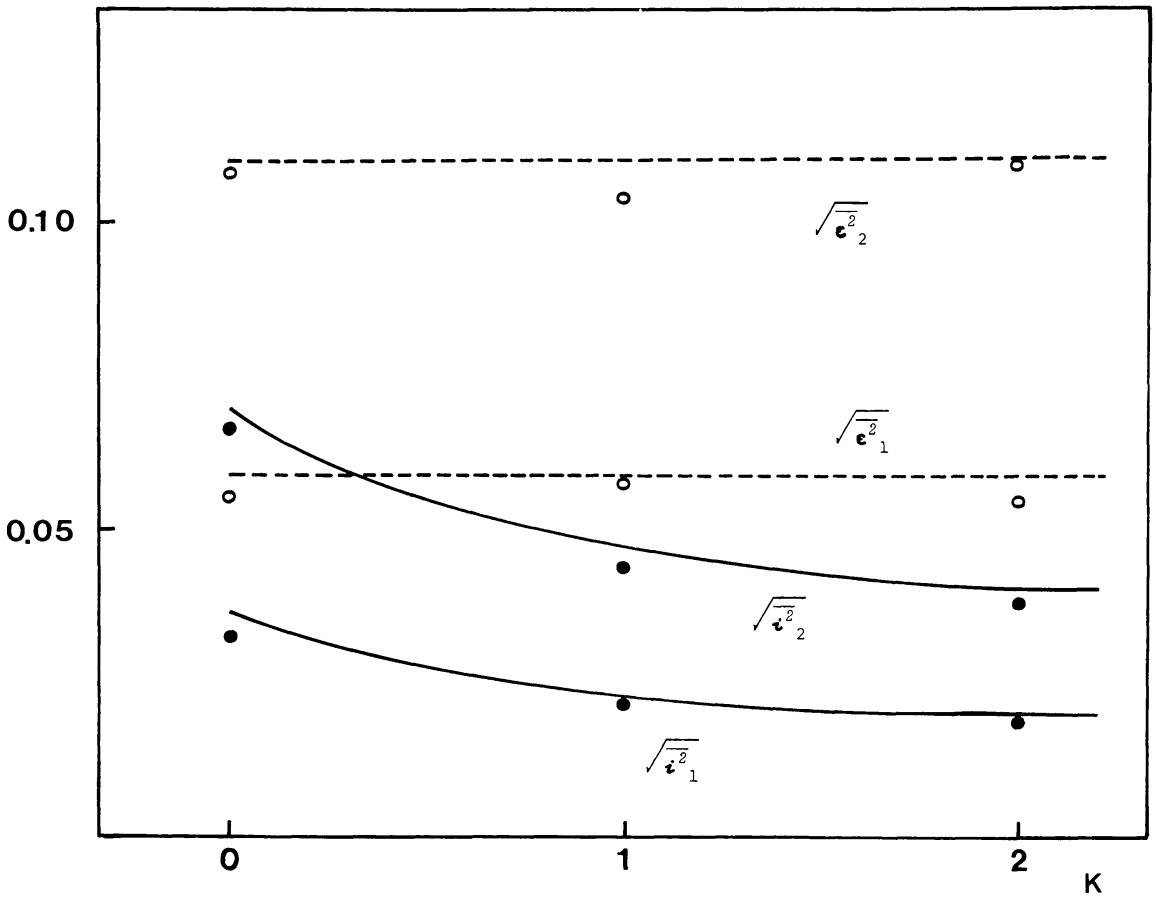

Fig. 4. The influence of an additional vertical force on the steady-state inclinations and eccentricities. Theoretical curves for $\sqrt{i^2}$ and $\sqrt{\epsilon^2}$ are drawn with solid and dashed lines, respectively. Gravitational encounters are included, $\mu_1 = 2 \times 10^{-5}$ and $\mu_2 = 0.25 \times 10^{-5}$. Other parameters are the same as in Figure 1.

on the adopted functional form of $\alpha(v)$, and also on the importance of finite particle size and gravitational encounters. These factors are now examined.

Figure 5 shows the results of three simulations made with $q = 2$ and $\mu_b/\mu_a = 2^6$, 2^9, and 2^{12}. The radius of the largest particle is 0.01, and $v_0 = 0.15$. The particles were divided into six mass-groups, and for each group the average mass and total optical thickness were calculated. The theoretical curves were constructed by replacing the continuous distribution with these six representative average values. The widest adopted distribution is near the upper limit for an accurate simulation of impacts: $\mu_b/\mu_a = 2^{12}$ yields $\sigma_b/\sigma_a = 16$, and the largest possible error at the impact distance is thus about 7% of σ_a (1% of the sum of the radii of colliding bodies). A larger width of size-distribution would also mean a very low total optical thickness and the formation of collisionless orbits could follow (this was actually observed in a rejected test run made with $\mu_b/\mu_a = 2^{18}$). The values of $\sqrt{T}$ and μT are constructed from the average values of $\sqrt{\epsilon^2}$ and $\sqrt{i^2}$ over the last 2000 impacts. The concentration of energy on large particles is very clear with $\mu_b/\mu_a = 2^9$ or 2^{12}.

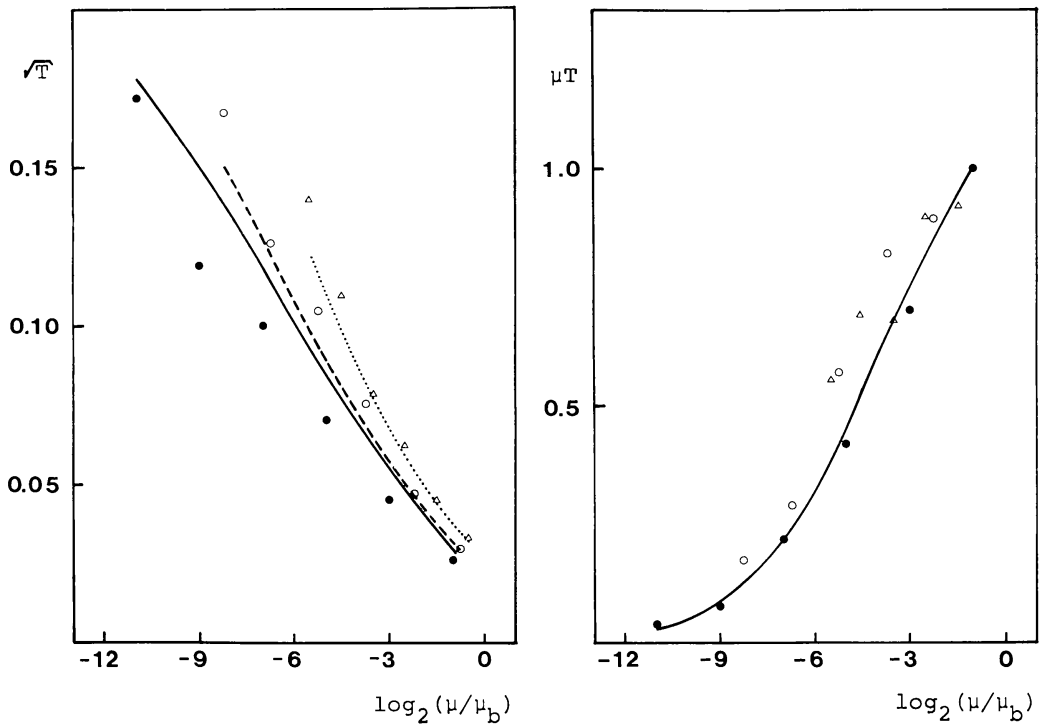

Fig. 5. The observed and theoretical distribution of $\sqrt{T}$ and μT versus particle mass in simulations with $\mu_b/\mu_a = 2^{12}$ (solid lines, filled circles), 2^9 (dashed lines, open circles), and 2^6 (dotted lines, triangles). The values of μT are plotted relative to those of the largest particles. The theoretical curve of μT is shown only for $\mu_b/\mu_a = 2^{12}$, the other two being almost identical to it. The power-index $q = 2$, $v_0 = 0.15$, and $\sigma_b = 0.01$. The gravitational encounters are not included.

Figure 6 shows the influence of q. While $q = 1$, the number of particles in each mass-group is constant, while with $q = 3$ the total optical thickness is the same in each group. Owing to the restricted number of particles, larger values cannot be studied. According to Figure 6 the increase in the relative number of small particles reduces the velocity dispersion of larger ones. This was also observed in those simulations of Paper I in which the relative optical thickness of small and large particles was varied in a system with two particle types.

The precise functional form of α is not crucial for the steady-state of the system, as long as $\alpha(\mathbf{v})$ is a decreasing function of impact velocity. This is evident from the simulations made with a more general function for α, namely

$$\alpha = 1/\{1 + (|c \cdot v|/v_0)^b\}, \qquad v_0, b = \text{const.} \tag{3}$$

In two simulations, with $b = 0.5$ and 2, respectively, a 50% difference in the velocity dispersions of smallest particles was observed (Figure 7). The functional form of $\alpha(\mathbf{v})$ chiefly affects the rate at which the system adjusts itself to the steady state. The smaller value of $|d\alpha/dv|$ ($b = 0.5$) slows the process and the final state is more sensitive to fluctuations.

In all of the above-mentioned simulations the free parameters in $\alpha(\mathbf{v})$ were chosen in

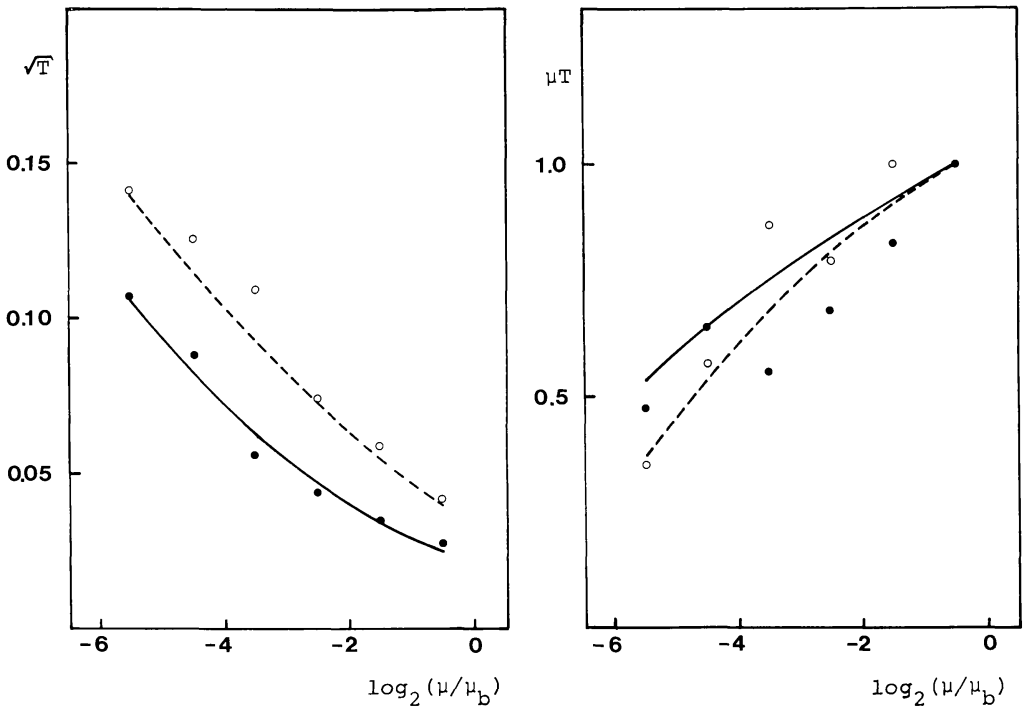

Fig. 6. Same as Figure 5, but different values of q are studied while $\mu_b/\mu_a = 2^6$. The case $q = 3$ is shown by solid lines and filled circles while the dashed lines and open circles correspond to $q = 1$.

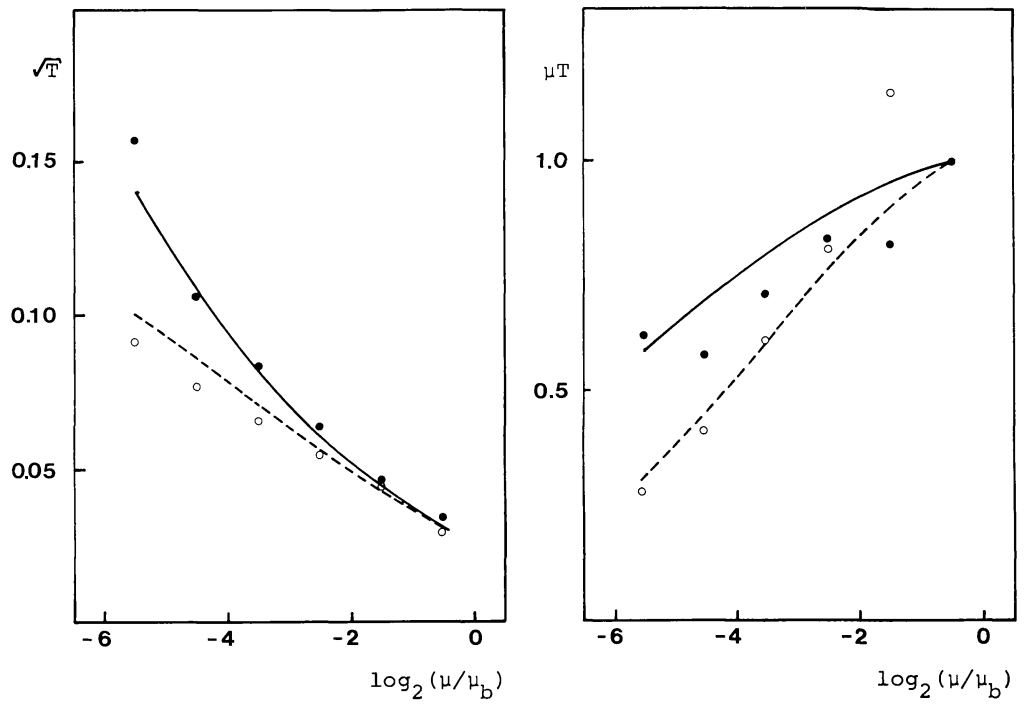

Fig. 7. Same as Figure 5 with $\mu_b/\mu_a = 2^6$. Equation (3) is used for $\alpha(v)$ with $b = 2$, $v_0 = 0.095$ (solid lines, filled circles) and with $b = 0.5$, $v_0 = 0.329$ (dashed lines, open circles).

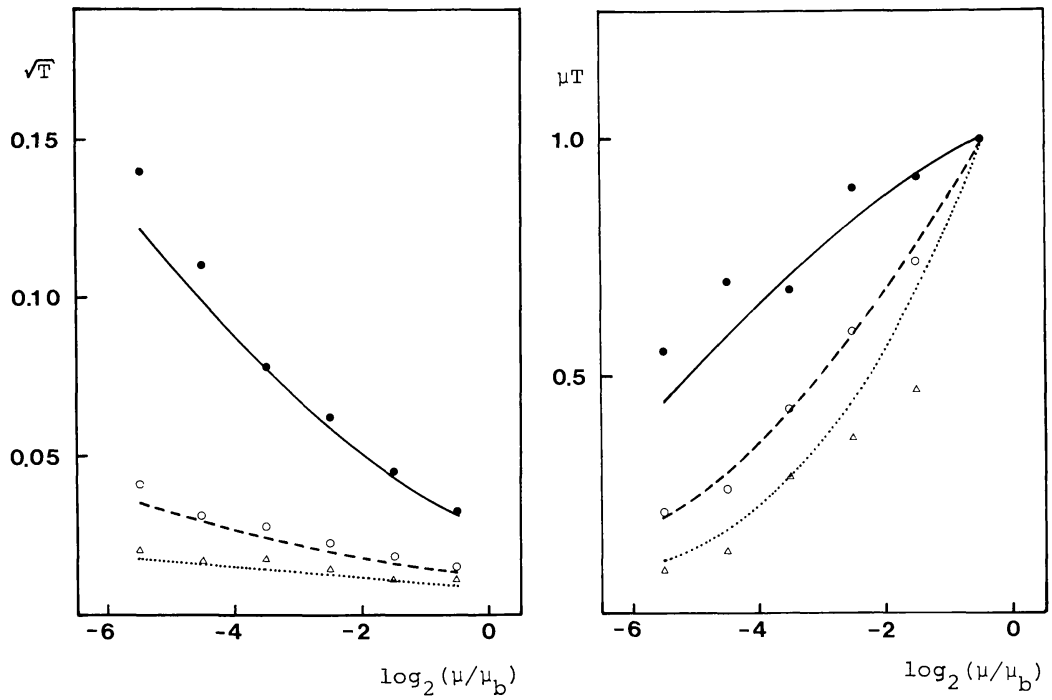

Fig. 8. Same as Figure 5, but different values of v_0 are used while $\mu_b/\mu_a = 2^6$. Simulations were made with $v_0 = 0.15$ (solid lines, filled circles), 0.025 (dashed lines, open circles), and 0.005 (dotted lines, triangles).

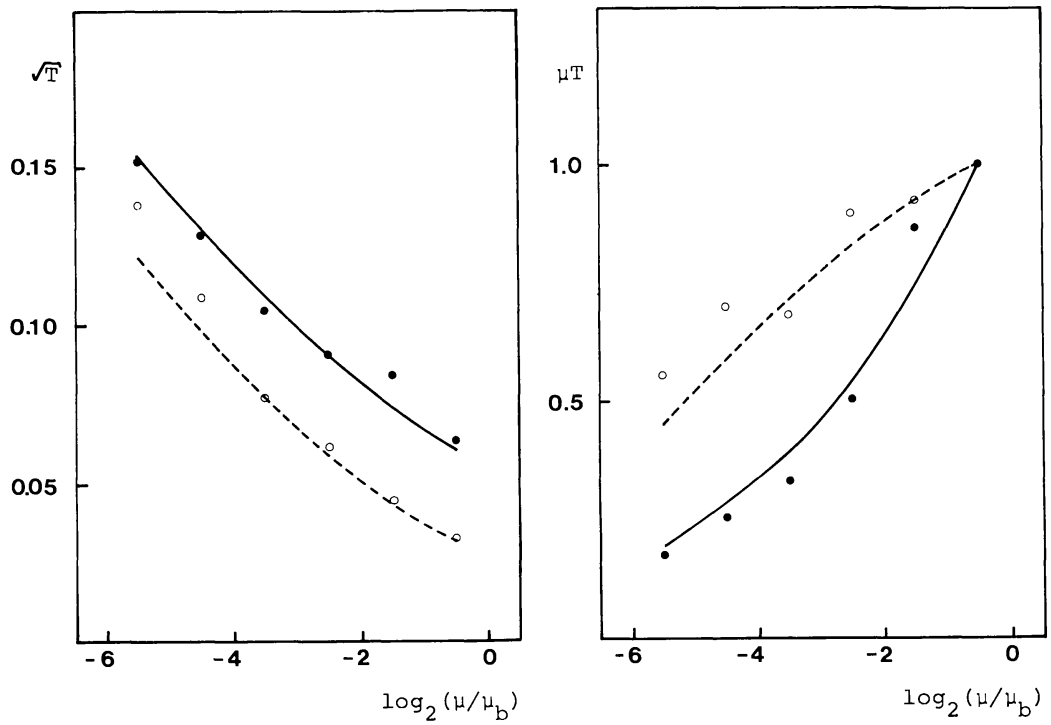

Fig. 9. Same as Figure 5 with $\mu_b/\mu_a = 2^6$. The distribution of $\sqrt{T}$ and μT is plotted with ($\mu_b = 5 \times 10^{-5}$, solid lines, filled circles) and without (dashed lines, open circles) gravitational encounters.

such a manner that the equilibrium values of inclinations and eccentricities were essentially larger than the particle radius. In this case the systematic velocity gradient, caused by the differential rotation, was insignificant. On the other hand, if the elastic properties of particles were such that the total velocity dispersion was mostly due to the finite size of colliding particles, a totally different distribution of $\sqrt{T}$ and μT was obtained. This is demonstrated in Figure 8 where the influence of finite particle size is emphasized by using smaller values of v_0. The values of $\sqrt{T}$ for the smallest particles are only slightly larger than those of the largest particles. This result resembles that obtained in the case $\alpha =$ constant (Paper I). The same result would also be achieved by using a systematically larger σ while v_0 is kept fixed.

The effects of gravitational encounters (Figure 9) are rather similar to those of the finite particle size. In general, the velocity dispersions of all particle types tend to increase by almost a constant amount (at least over the limited mass-range studied) and thus the relative share of random kinetic energy of large particles increases.

5. Application to the Rings of Saturn

Due to the restricted width of the size-distribution in simulations, the direct extrapolation of the results to real systems would be questionable. However, if these are combined with theoretical equations (Hämeen-Anttila, 1984), rather reliable estimates can be made. In this section the velocity dispersion of the rarefied regions of Saturn's rings is examined.

In earlier studies (Hämeen-Anttila, 1982, 1983; Salo and Lukkari, 1982; Salo, 1984) the models proposed for Saturn's rings were based on the assumption that the observed edge-on thickness of the ring system is due to the large dispersion of velocities in rarefied regions. This assumption fixed the unknown parameter v_0 in Equation (1). The application of the theoretical equations of identical particles then indicated that values of $v_0 \simeq 1\ \mathrm{m\,s^{-1}}$ were needed in order to yield the measured (Brahic and Sicardy, 1981) effective thickness $h \simeq 1.4$ km at the Saturnocentric distance $r = 10^5$ km. Since there are now laboratory measurements available (Bridges *et al.*, 1984), the use of an arbitrary model function is unnecessary, and can be replaced with that derived directly from relevant observations (if we assume that the particles consist of pure ice). Bridges *et al.* (1984) found that their results agree very well with the power law

$$\alpha = (0.32 \pm 0.02) V^{-0.234 \pm 0.008}, \quad \text{if} \quad 0.015 < V < 5.1, \tag{4}$$

where V is the impact velocity in units of $\mathrm{cm\,s^{-1}}$. Although having a different functional form, our Equation (3) with $b = 0.5$ and $v_0 = 0.15\ \mathrm{cm\,s^{-1}}$ is very close to this function. The low value of v_0 suggests a strongly flattened system. Bridges *et al.* (1984) applied their measurements to Saturn's rings and derived an upper bound $h < 5$ m, by assuming that all particles are identical with $\sigma \ll 5$ m. However, the finite particle size and gravitational encounters, together with the wide distribution of sizes is likely to increase h.

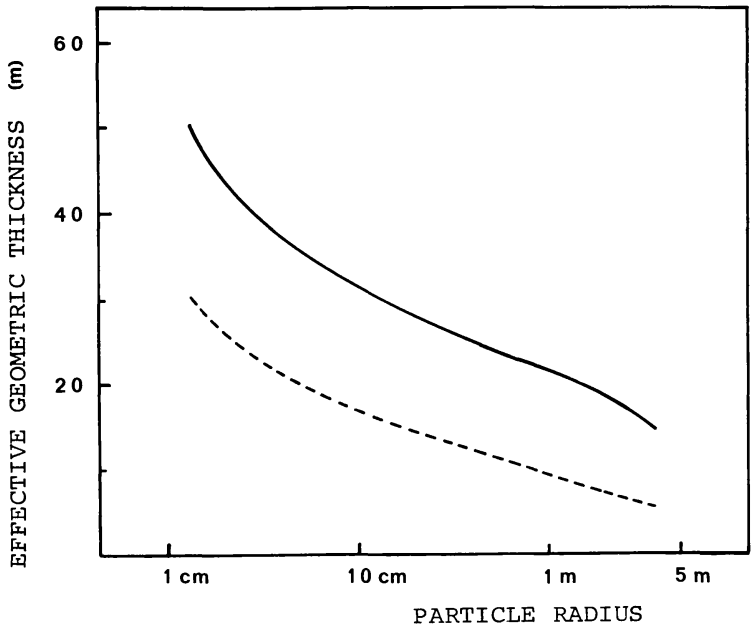

Fig. 10. The theoretical geometric thickness of rarefied regions at the Saturnocentric distance of 10^5 km with (solid line) and without (dashed line) gravitational encounters. The distribution of sizes extends from 1 cm to 5 m, and $q = 3$. Equation (4) is used for $\alpha(\mathbf{v})$, and the internal density of particles is assumed to be 0.9 g cm^{-3}.

According to the simulations of Figure 8 the agreement between theory and simulations is good even if a large part of the velocity dispersion is induced by differential rotation. If the observed value of v_0 for ice is scaled to our simulation units ($\sigma = 0.01$), the particle radius $\sigma = 5$ m (at the distance of 10^5 km) corresponds to $v_0 = 0.0154$ in Equation (1). Thus the parameter range of Figure 8 should be relevant as compared with the actual elastic properties of ring particles. The maximum deviation between theory and simulations is about 20%, but there seems to be no systematic increase of error towards the small-particle limit of size-distribution. According to the simulations with a large width of the size-distribution (Figure 5, $\mu_b/\mu_a = 2^{12}$) the theoretically predicted ϵ and i are slightly larger than the actually observed values. However, the difference is again less than 20%.

Figure 10 presents the calculated effective thickness of rarefied regions at a Saturnocentric distance of 10^5 km. The coefficient of restitution is assumed to be of the form of Equation (4), and the distribution of sizes extends from 1 cm to 5 meters, with a power-index $q = 3$. This is in accordance with the analysis of Voyager 1 radio occultation measurements (Marouf *et al.*, 1983). According to Figure 10 the velocity dispersion and the following effective geometric thickness, $h \simeq r\sqrt{6i^2}$ (Hämeen-Anttila, 1983), of the smallest particles is considerably larger than the above-mentioned estimate for identical mass-points. The upper curve of Figure 10, including the effects of gravitational encounters, must be considered only tentative, since the average post-collisional velocity in impacts involving largest m-sized particles drops below the escape velocity. This would

mean a continuous growth of loose, gravitationally bound particle aggregates, which is not taken into account in the construction of Figure 10. However, it seems certain that Figure 10 describes in a qualitatively correct way the influence of encounters.

5. Conclusions

According to the present simulations there seems to be good agreement between numerical experiments and Hämeen-Anttila's (1984) theory, both in the case of Keplerian and self-gravitating systems of non-identical particles. Due to the rapid dispersal of simulation systems, together with large statistical fluctuations, an exact comparison of local velocity dispersions is not possible. In encounter simulations with large particle masses the average post-collisional velocity falls below the escape velocity, thus leading to a formation of particle groups. This violates the limitations of the collisional theory and even qualitative comparison is no longer possible.

The simulations made with a continuous power-law distribution of sizes indicate that both the width of the distribution and the value of power-index q affect the distribution of velocities versus particle mass. An increase in the relative number of small particles, achieved either by using a larger μ_b/μ_a or a larger q, reduces the velocities of all particle sizes. If the elastic properties of particles are such that α drops to a low level even with a small impact velocity (v_0 is small) the corresponding steady-state dispersion of velocities would be very small. Therefore, the finite particle size becomes dominant in maintaining the velocity dispersion. The form of the velocity distribution, controlled by $\alpha(v)$-relation or by finite particle size is different: in the latter case the random velocities of small particles are closer to those of the large ones. The influence of gravitational encounters resembles that of increased particle size.

The estimations made for the effective geometric thickness of rarefied regions in Saturn's rings indicate that the inclusion of the size distribution and gravitational encounters increase the predicted thickness above the value which corresponds to identical non-gravitating mass-points. Without encounters the effective thickness of the layer of cm-sized particles becomes about 30 m, and the inclusion of them raises it to 50 m, mainly because the velocity dispersion of the largest particles is increased.

References

Brahic, A. and Sicardy, B.: 1981, *Nature* **289**, 447.
Bridges, F. G., Hatzes, A., and Lin, D. N. C.: 1984, *Nature* **309**, 333.
Hämeen-Anttila, K. A.: 1982, *The Moon and Planets* **26**, 171.
Hämeen-Anttila, K. A.: 1983, *The Moon and Planets* **28**, 267.
Hämeen-Anttila, K. A.: 1984, *Earth, Moon, and Planets* **31**, 271.
Hämeen-Anttila, K. A. and Lukkari, J.: 1980, *Astrophys. Space Sci.* **71**, 475.
Lukkari, J. and Salo, H.: 1984, *Earth, Moon, and Planets* **31**, 1.
Marouf, E. A., Tyler, G. L., Zebker, H. A., Simpson, R. A., and Eshleman, V. R.: 1983, *Icarus* **55**, 439.
Salo, H.: 1984, *Earth, Moon, and Planets* **30**, 113.
Salo, H. and Lukkari, J.: 1982, *The Moon and Planets* **27**, 5.
Salo, H. and Lukkari, J.: 1984, *Earth, Moon, and Planets* **30**, 229.